Journal of Sound and Vibration (1999) **220**(3), 497–516
Article No. jsvi.1998.1963, available online at http://www.idealibrary.com on IDEAL

THE IN-PLANE VIBRATION OF THIN RINGS WITH IN-PLANE PROFILE VARIATIONS PART I: GENERAL BACKGROUND AND THEORETICAL FORMULATION

R. S. Hwang, C. H. J. Fox and S. McWilliam

Department of Mechanical Engineering, University of Nottingham, University Park, Nottingham NG7 2RD, UK

(*Received* 24 *February* 1998, *and in final form* 7 *September* 1998)

This paper presents a methodology for the analysis of the free, in-plane, vibration of thin rings with profile variations in the circumferential direction. The methodology is suitable for any thin ring which is bounded by closed curves which are single valued functions of circumferential position. The inner and outer profiles are expressed as Fourier series, thus allowing any profile to be approximated with any degree of accuracy. An iterative numerical procedure for determining the true middle surface and the corresponding thickness at each cross-section around the circumference is established. A reduced (plane stress) form of Novozhilov's thin-shell theory is used to model the deformation mechanics of the ring. The eigenvalue problem is then formulated using the Rayleigh–Ritz method in conjunction with a harmonic series description of the displacements. General expressions are presented for the corresponding mass and stiffness matrices. A companion paper presents a comprehensive set of results which illustrates application of the theory.

1. INTRODUCTION

The free vibration of rings and cylindrical shells has been widely studied for over a century. Much of the early work on rings is summarised in reference [1] while reference [2] contains a comprehensive survey of work completed prior to 1973 on the vibration of shells. More recent work of particular relevance to the present paper will be reviewed later.

The great majority of papers dealing with rings and cylindrical shells are restricted to cases where the structure is either perfectly circular, or has a non-circular but otherwise perfectly defined shape such as an ellipse. However, such perfect shapes are impossible to realise in practice due to limitations in manufacturing processes which cause departures from the nominal profile, i.e., imperfection.

The general effects of imperfection on the natural frequencies and mode shapes of nominally circular rings and cylinders is well understood [3]. In particular,

0022–460X/99/080497 + 20 $30.00/0

imperfection causes frequency splitting between pairs of modes which would, in a perfectly circular structure, have identical natural frequencies. It also fixes the nodal positions in the structure, thus removing the circumferential indeterminacy which exists in perfectly axi-symmetric structures.

The initial reason for carrying out the work reported in the present paper was to obtain an improved *quantitative* understanding of the effects on natural frequencies and mode shapes of small derivations from true circularity in rings and cylinders. This was motivated by the involvement of the authors in the development of inertial sensors (rate gyroscopes and rate integrating gyroscopes) which use a vibrating ring or cylinder as their sensitive element [4, 5]. In these applications, frequency splitting of the order of 100 ppm (0·01%) or better is often required between the relevant modes which are usually low order (''2θ'' or ''3θ'') radial modes. Thus, levels of imperfection which would be irrelevant in many structures assume a first order importance in such applications.

The most important early work on the free vibration of a circular ring [6] was published in 1871 by Hoppe, who obtained a simple classical solution by neglecting the effects of centreline extension, shear deformation and rotatory inertia. Subsequently, many authors have investigated the vibration of thin rings and shells [1, 2] using a variety of methods based on either Newtonian or energy approaches.

Regarding rings, the majority of papers deal with structures which are either perfectly circular or perfectly elliptical with a circumferentially constant cross-section. Comprehensive reviews of these are given in references [7, 8]. Relatively few papers deal with the more general case where the ring cross-section shape varies with circumferential position and a brief review of the most important of these follows.

References [9, 10] presented analyses of the vibrations of circular and non-circular rings and shells. In these, the shape of the mid-surface was assumed to be a simple analytic function of the circumferential co-ordinate and the circumferential variation in ring thickness and the ring deformation were both described using ''infinite'' power series (truncated in practice at 90 terms). This approach would be difficult to apply to rings of arbitrary profile for which the mid-surface shape is not known *a priori* in a suitable form.

In references [11, 12], rings were treated as one-dimensional curved beams to investigate the in-plane vibrations of rings of non-uniform cross-section in which specific forms of the centreline of the middle surface were assumed. Exact solutions for the axi-symmetric modes of vibrating rings of uniform cross-section were used as the basis for approximate solutions for rings with non-uniform cross-section, using a first order approximation based on beam bending theory.

The effects of simple eccentricity in circular rings were considered in reference [13], which presented a perturbation analysis in which the classical frequency equation for a thin ring is modified to account for eccentricity, and frequency splitting was predicted.

The analysis presented in reference [14] is of particular relevance to the work reported in the present paper. Reference [14] deals with circular cylindrical shells with circumferential thickness variation caused by eccentricity between circular inner and outer surfaces. The shell geometry was defined by two circular profiles

with non-coincident centres. The cylinder centre was taken to be midway between the centres of the inner and outer surfaces and the thickness variation was represented by Fourier series. Love's thin shell theory and the Rayleigh–Ritz method were used to estimate the natural frequencies and frequency splitting. An important assumption on which the analysis in reference [14] is based is that there exists an unstrained *circular* mid-surface which is taken to be a circle whose radius is the mean of the radii of the inner and outer surfaces. Strictly speaking this does not comply with the formal definition [15] of the mid-surface which is taken as the locus of points which lie at equal distances from the inner and outer surfaces along the directions of the normal to the mid-surface. The accuracy of results based on the analysis given in reference [14] will therefore be affected by the assumed definition of mid-surface, although for small eccentricity in thin rings the effect may be expected to be minimal. However, for profiles which are far from having a circular mid-surface (such as ellipses, ovals and polygons) the assumption of a circular mid-surface is not valid. The present paper presents a methodology for the formulation of the eigenvalue problem for the in-plane vibration of thin, flat rings of constant axial length with variable radius and circumferentially variable rectangular cross-section as considered in reference [7]. The shape of the ring is defined by two closed profiles, each of which is a single-valued function in polar co-ordinates. The inner and outer profiles are decomposed as Fourier series, thus allowing any single-valued profile to be approximated to any desired degree of accuracy in a very general way. It may be noted that modern metrology equipment for measuring circularity can be used to provide the required Fourier series description of any such machined profile.

The middle surface of the ring is properly determined from the inner and outer surfaces in accordance with the usual definition [15], using an iterative numerical procedure. A reduced, plane stress version of Novozhilov's thin shell theory is used to describe the deformation mechanics of the ring. Novozhilov's theory is often regarded [16, 17] as being the most accurate for shells of arbitrary shape.

Finally, the Rayleigh–Ritz method is used to set up the eigenvalue problem in terms of generalised co-ordinates which are taken to be the harmonic displacement functions of the flexural vibration of a perfect ring.

It may be noted that the method used in the present paper could be extended to cover the vibration of prismatic thin shells with circumferentially variable thickness.

The Fourier series description of the ring geometry adopted here is obviously appropriate for rings which are nominally circular. It is, however, equally suitable for other closed shapes such as ellipses, ovals and polygons. A companion paper [18] reports the application of the methodology of the present paper to a range of rings of nominally circular shape, and draws conclusions about the effects of simple departures from circularity in the inner and outer profiles. A further paper [19] will present results for elliptical rings, with and without circumferential thickness variations.

Before the vibration analysis can be carried out it is first necessary to devise a logical system for describing the inner and outer profiles of the ring, and for

determining the true middle surface. These issues are addressed in sections 2.1 and 2.2 below.

2. GEOMETRY AND IMPERFECTION

2.1. RING GEOMETRY

Consider a thin ring of mean radius r_a having a rectangular cross-section of mean thickness h ($\ll r_a$) and axial length L ($\ll r_a$). The inner and outer surfaces vary circumferentially. Two co-ordinate systems are used to formulate the problem, as follows (see Figure 1): (1) Global polar co-ordinates in which unit vectors $\imath_{\beta'}$, $\imath_{\xi'}$ are directed along the global circumferential and radial directions. The initial geometry of the undeformed ring is defined using this co-ordinate system; (2) Local curvilinear co-ordinates in which unit vectors $\imath_\beta$, $\imath_\xi$ are directed along the local tangential and normal directions relative to the middle surface which is yet to be determined. This local co-ordinate system is required for deriving the strain and kinetic energies, based on the Novozhilov thin-shell theory, in terms of radial and circumferential displacements which are w, v in the local co-ordinate system (and w', v' in the corresponding global co-ordinate system). In Figure 1, r_P denotes the distance from an arbitrary fixed point C' inside the ring to a general point P located on the middle surface at angle β' relative to an arbitrary datum in global co-ordinate and θ_P is the angle between the global and local co-ordinate systems at the point P. In the following formulation, all the displacements, thicknesses, and radii are expressed non-dimensionally by dividing by r_a, the mean radius of the ring.

The overall geometry of the ring is determined by the shape of the inner and outer bounding surfaces which, in turn, determine the position and shape of the middle surface of the ring (see Figure 2). This contrasts with other formulations

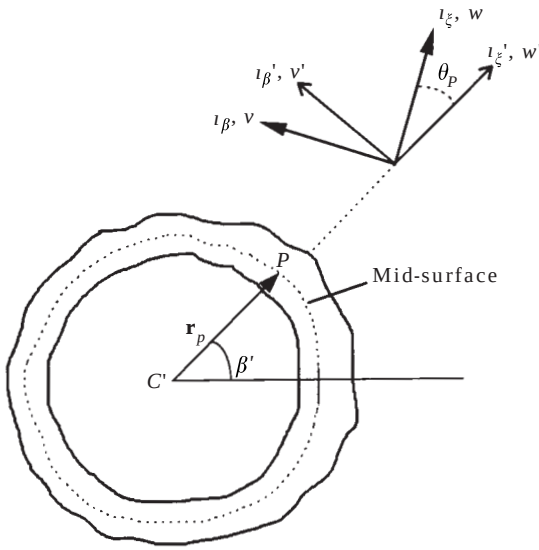

Figure 1. A thin ring with arbitrary profile.

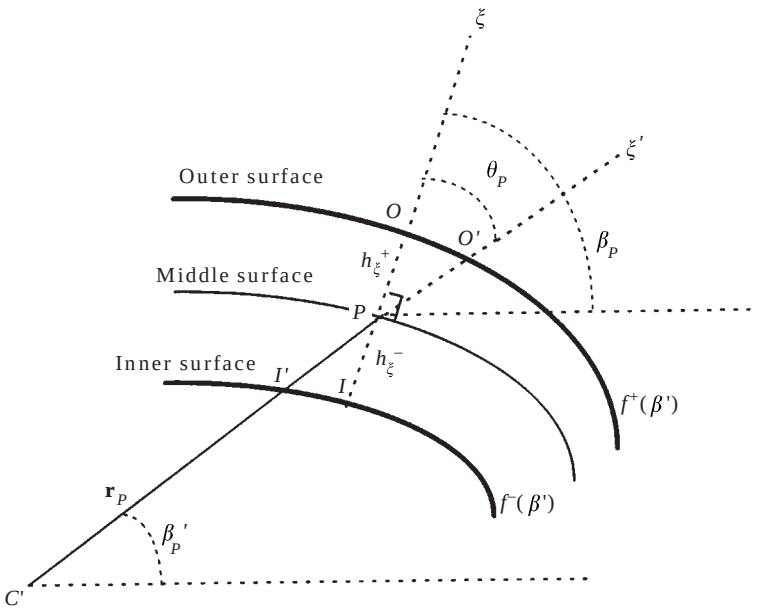

Figure 2. The bounding surfaces and the middle surface.

where the shape of the mid-surface is assumed to be known *a priori*. Due to the fact that they are (single valued) closed curves, the outer and inner surfaces can be expressed by Fourier series in terms of the global circumferential co-ordinate β' as follows:

$$f^{+}(\beta') = f_0^{+} + \sum_{p=1}^{n} f_p^{+} \cos(p\beta') + \sum_{q=1}^{n} f_q^{+} \sin(q\beta'), \tag{1}$$

$$f^{-}(\beta') = f_0^{-} + \sum_{p=1}^{n} f_p^{-} \cos(p\beta') + \sum_{q=1}^{n} f_q^{-} \sin(q\beta'), \tag{2}$$

where $f^{+}(\beta')$ and $f^{-}(\beta')$ denote respectively the outer and inner surface profile functions with respect to the global circumferential co-ordinate β' and $f_0^{+}, f_p^{+}, f_q^{+}$, f_0^{-}, f_p^{-} and f_q^{-} are the Fourier coefficients. In practice, the Fourier coefficients can be measured by suitable metrology equipment. In Figure 2, $f^{+}(\beta')$ and $f^{-}(\beta')$ denote respectively the distance from arbitrary point C' to points O' and I' on the outer and inner surfaces. Choosing C' at a different position will lead to a different set of Fourier coefficients for the same inner and outer profiles. Note however that the choice of C' must be the same for both inner and outer profiles.

2.2. DETERMINATION OF THE MIDDLE SURFACE

The middle surface is defined as the locus of points which lie at equal distances from the outer and inner surfaces along the direction normal to the mid-surface. Thus, referring to Figure 2 the thickness at a point P on the true middle surface is equal to the distance $\overline{IO}$ measured along the local normal direction ξ. Hence,

since point P lies on the middle surface, we have $h_\xi^+ = h_\xi^-$, where h_ξ^+ and h_ξ^- denote the outer and inner thicknesses measured from the point P to the outer and inner surfaces along the local normal direction ξ.

The problem now is to determine the position of the true mid-surface, given the inner and outer profiles which define the ring. This can be achieved using an iterative procedure as described below. Consider first Figure 3(a) which shows the inner and outer profiles $f^-(\beta_P')$ and $f^+(\beta_2')$.

I' and O' are points on the inner and outer surfaces along the global radial direction ξ' at a given orientation β_P' which corresponds to point P on the true mid-surface. I and O are points on the inner and outer surfaces along the local normal to the middle surface at P. $\overline{C'I}$ and $\overline{C'O}$ are the inner and outer surface profile functions, $f^-(\beta_1')$ and $f^+(\beta_2')$, evaluated at orientations β_1' and β_2', respectively, which are to be determined. r_P is the length of a vector, $\mathbf{r}_P$, from C' to the point P on the middle surface, and θ_P denotes the angle between the local and global co-ordinate systems so that $\beta_P = \beta_P' + \theta_P$.

For a given orientation β_P', the outer and inner surface functions, $f^+(\beta_P')$ and $f^-(\beta_P')$, are known and are defined by equations (1) and (2) but $\mathbf{r}_P$ is unknown initially. From the definition of middle surface and Figure 3(a), the length of $\mathbf{r}_P$ at global position β_P' can be expressed in terms of $f^+(\beta_P'), f^-(\beta_P')$ and variable parameter m as follows

$$r_P = mf^+(\beta_P') + (1 - m)f^-(\beta_P'), \tag{3}$$

where $0 < m < 1$. In general, m will vary as β_P' changes. In the special case where $f^+(\beta_P')$ and $f^-(\beta_P')$ are concentric circles, $m = 0{\cdot}5$.

The true middle surface can now be determined using the following iterative numerical procedure.

Step I—Assume initially that P on the middle surface at orientation β_P', is also the mid-point of $I'O'$ (i.e., $\overline{I'P} = \overline{PO'}$), and $m = 0{\cdot}5$ in equation (3).

Step II—Determine the corresponding locations of I and O in terms of the given orientation β_P'.

To do this, it is necessary to note that, from geometrical considerations (see Figure 3(b))

$$\begin{aligned}\tan \beta_P &= \overline{Q_1P}/\overline{IQ_1} = [\overline{PM} - \overline{IB}]/[\overline{C'M} - \overline{C'B}] \\ &= [\overline{C'P} \sin \beta_P' - \overline{C'I} \sin \beta_1']/[\overline{C'P} \cos \beta_P' - \overline{C'I} \cos \beta_1'],\end{aligned} \tag{4}$$

and, similarly (see Figure 3(c))

$$\begin{aligned}\tan \beta_P &= \overline{Q_2O}/\overline{PQ_2} = [\overline{OD} - \overline{PM}]/[\overline{C'D} - \overline{C'M}] \\ &= [\overline{C'O} \sin \beta_2' - \overline{C'P} \sin \beta_P']/[\overline{C'O} \cos \beta_2' - \overline{C'P} \cos \beta_P'],\end{aligned} \tag{5}$$

where (see Figure 3(a))

$$\beta_P = \beta_P' + \theta_P. \tag{6}$$

Starting from the definition of curvature [20] it can be shown [7] that θ_P can be expressed as

$$\theta_P = \tan^{-1} \frac{-\dot{r}_p}{|r_p|}. \tag{7}$$

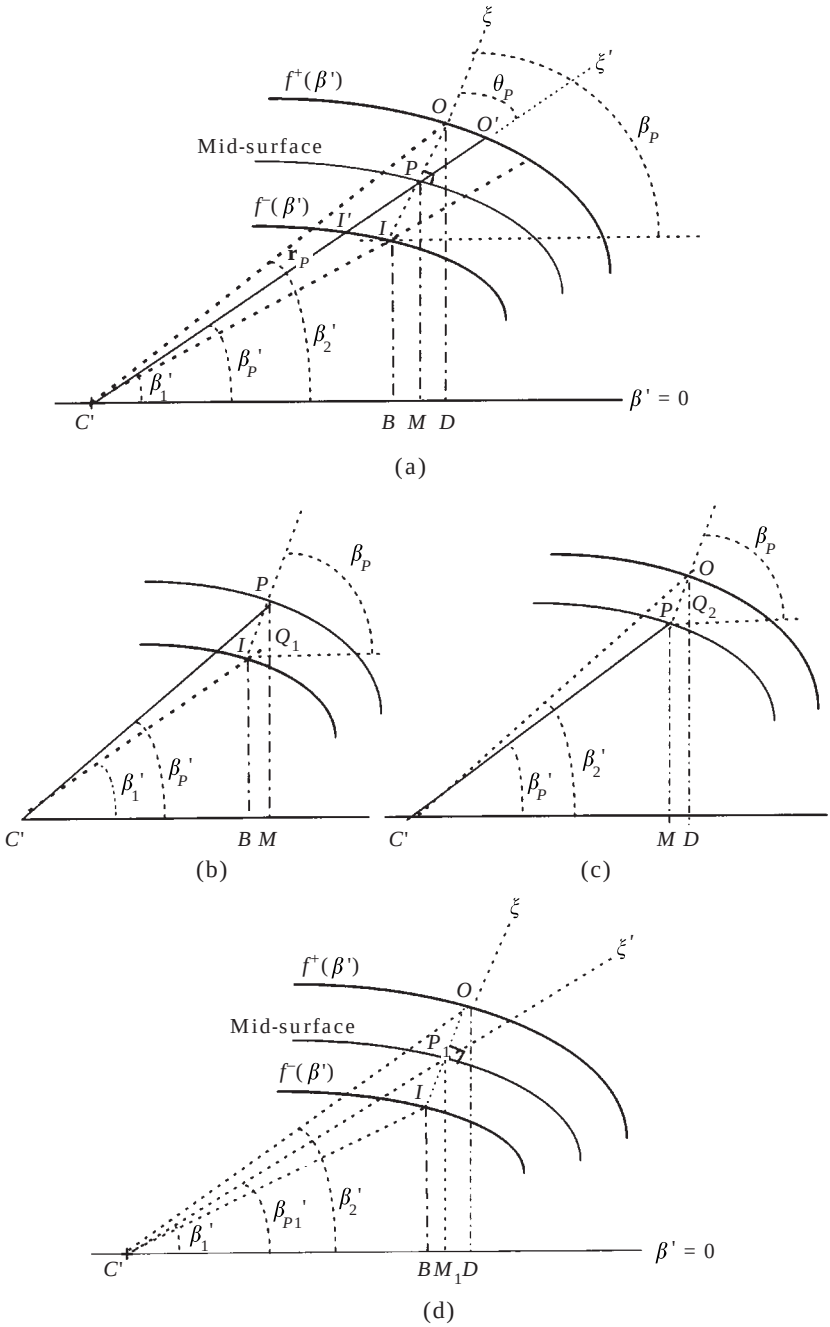

Figure 3. The determination of the middle surface of a ring. (a) The assumed middle surface. (d) The true middle surface ($IP_1 = P_1O$).

Note that $\dot{r}_p$ denotes the first derivative of r_p (defined by equation (3)) with respect to β'_P.

Substitution of equations (3), (6) and (7) into equation (4) gives:

$$\tan(\beta'_P + \theta_P) = \{[mf^+(\beta'_P) + (1-m)f^-(\beta'_P)]\sin\beta'_P - f^-(\beta'_1)\sin\beta'_1\} / \{[mf^+(\beta'_P) + (1-m)f^-(\beta'_P)]\cos\beta'_P - f^-(\beta'_1)\cos\beta'_1\}. \quad (8)$$

Similarly, equation (5) can be rewritten as

$$\tan(\beta'_P + \theta_P) = \{f^+(\beta'_2)\sin\beta'_2 - [mf^+(\beta'_P) + (1-m)f^-(\beta'_P)]\sin\beta'_P\} / \{f^+(\beta'_2)\cos\beta'_2 - [mf^+(\beta'_P) + (1-m)f^-(\beta'_P)]\cos\beta'_P\}. \quad (9)$$

Noting the definition of θ_P using equations (7) and (3), inspection of equations (8) and (9) indicates that β'_1 and β'_2 are the only unknown variables when m takes an assumed value. A standard numerical technique, such as the Newton–Raphson method, can be used to solve these non-linear equations for the unknown variables. Having obtained β'_1 and β'_2, the corresponding locations of I and O can be determined.

Step III—Determine the mid-point P_1 between the inner and outer surfaces along the line $\overline{IO}$ (see Figure 3(d).

From Figure 3(d), it can be seen that

$$\overline{C'P_1} = \frac{\overline{C'M_1}}{\cos\beta'_{P_1}} = \frac{\frac{1}{2}(\overline{C'D} + \overline{C'B})}{\cos\beta'_{P_1}} = \frac{\overline{C'O}\cos\beta'_2 + \overline{C'I}\cos\beta'_1}{2\cos\beta'_{P_1}}, \quad (10)$$

where

$$\beta'_{P_1} = \tan^{-1}\frac{\overline{P_1M_1}}{\overline{C'M_1}} = \tan^{-1}\frac{\frac{1}{2}(\overline{OD} + \overline{IB})}{\frac{1}{2}(\overline{C'D} + \overline{C'B})}$$

$$= \tan^{-1}\frac{\overline{C'O}\sin\beta'_2 + \overline{C'I}\sin\beta'_1}{\overline{C'O}\cos\beta'_2 + \overline{C'I}\cos\beta'_1}. \quad (11)$$

Equations (10) and (11) can be solved using the Newton–Raphson numerical method to obtain β'_{P1}, the angular position of point P_1.

The positional difference between the originally assumed mid-point P and the newly estimated mid-point P_1 is then compared to a given tolerance in terms of the global circumferential co-ordinate ($1{\cdot}0 \times 10^{-5}$ rad was used to ensure four significant figures in the frequencies in the numerical investigations [7, 18, 19].

Step IV—If P and P_1 do not coincide within the given tolerance, then repeat steps II and III until the true mid-point is found.

At each iteration the point P is redefined by setting $r_P = \overline{C'P_1}$ for the same value of β'_P and m is recalculated from equation (3) where

$$m = [r_P - f^-(\beta'_P)]/[f^+(\beta'_P) - f^-(\beta'_P)]. \quad (12)$$

When the point P on the true middle surface is determined, the variables r_P, h_ξ^-, h_ξ^+, θ_P and β_P at the given β'_P can be calculated. The same iterative procedure can then be used to calculate all the corresponding variables section by section around the circumference from $\beta' = 0$ to 2π. The step length in β' should be varied depending on the complexity of the profile variation and the desired accuracy in the frequencies ($1{\cdot}0 \times 10^4$ rad was used for the small profile variations to achieve four significant figures frequency accuracy in the numerical investigations [7, 18, 19]).

Having defined the ring geometry it is necessary to derive expressions for the kinetic energy and strain energy of the deformed ring so that the Rayleigh–Ritz method can be applied. This will be done in the next section.

3. ENERGY EXPRESSIONS

The strain energy for a thin ring whose axial length is much smaller than the mean radius has the form [12]:

$$S = \frac{r_a^2 EL}{2} \int_{\beta_1}^{\beta_2} \int_{h_\xi^-(\beta)}^{h_\xi^+(\beta)} e_{\beta\beta}^2 R\left(1 + \frac{\xi}{R}\right) \mathrm{d}\beta \, \mathrm{d}\xi, \tag{13}$$

where r_a is the mean radius of the middle surface, which is taken as the zero order Fourier harmonic of the mid-surface profile. E is Young's modulus and L is the axial length of the ring. $e_{\beta\beta}$, the normal strain along the local tangential co-ordinate β, and R, the non-dimensional radius of curvature at a point on the middle surface, are functions of β'. R can be determined at point P using the following equation [20]:

$$\frac{1}{R} = \frac{\sqrt{(\dot{r} \cdot \dot{r})(\ddot{r} \cdot \ddot{r}) - (\dot{r} \cdot \ddot{r})^2}}{(\dot{r} \cdot \dot{r})^{3/2}}, \tag{14}$$

where $\mathbf{r} = \mathbf{r}_P$ as previously defined. Note that the limits of integration, h_ξ^+ and h_ξ^-, in equation (13) are functions of β'.

Based on the reduced Novozhilov thin-shell theory in which the plane-stress approximation is used by neglecting axial deformations and axial variations in radial and tangential displacements, the normal strain $e_{\beta\beta}$ in equation (13) is given as

$$e_{\beta\beta} = \frac{1}{1 + \xi/R} (\varepsilon_\beta + \xi \kappa_\beta), \tag{15}$$

where

$$\varepsilon_\beta = \frac{1}{R} \frac{\partial v}{\partial \beta} + \frac{w}{R}, \qquad \kappa_\beta = -\frac{1}{R} \frac{\partial}{\partial \beta} \left(\frac{1}{R} \frac{\partial w}{\partial \beta} - \frac{v}{R} \right). \tag{16, 17}$$

ε_β and κ_β characterise the deformation of the middle surface of the ring. ε_β is the tangential strain at the middle surface and κ_β is the change of curvature. v, w are the non-dimensional displacement components of a point on the middle surface along the tangential and normal directions respectively.

Substituting equations (14)–(17) into equation (13), then integrating with respect to the thickness from h_ξ^- to h_ξ^+, neglecting the 4th and higher powers of h_ξ^+ and h_ξ^- and noting that $\int_{\beta_1}^{\beta_2} F(\beta)[h_\xi^{+2} - h_\xi^{-2}]\,\mathrm{d}\beta = 0$ where $F(\beta)$ is an arbitrary function of β, the strain energy can be expressed in terms of the tangential and normal displacements, v and w, and local co-ordinate β as follows

$$S = \frac{r_a^2 EL}{2}\int_{\beta_1}^{\beta_2}\left\{\left[\frac{1}{R}\left(\frac{\partial v}{\partial\beta}\right)^2 + 2w\frac{\partial v}{\partial\beta} + w^2\right]H + \frac{1}{3R^3}\left[w^2 + 2w\frac{\partial^2 w}{\partial\beta^2} + \left(\frac{\partial^2 w}{\partial\beta^2}\right)^2\right]H^3 + \frac{1}{3R^2}\left[2w\frac{\partial w}{\partial\beta} + 2\frac{\partial w}{\partial\beta}\frac{\partial^2 w}{\partial\beta^2} - 2vw - 2v\frac{\partial^2 w}{\partial\beta^2}\right]\frac{\partial}{\partial\beta}\left(\frac{1}{R}\right)H^3 + \frac{1}{3R}\left[\left(\frac{\partial w}{\partial\beta}\right)^2 + v^2 - 2v\frac{\partial w}{\partial\beta}\right]\left[\frac{\partial}{\partial\beta}\left(\frac{1}{R}\right)\right]^2 H^3\right\}\mathrm{d}\beta, \tag{18}$$

where H and H^3 denote $(h_\xi^+ - h_\xi^-)$ and $(h_\xi^{+3} - h_\xi^{-3})$, respectively.

Similarly, the kinetic energy can be expressed as

$$T = \frac{r_a^4 \rho L}{2}\int_{\beta_1}^{\beta_2}\int_{h_\xi^-(\beta)}^{h_\xi^+(\beta)}\left[\left(\frac{\partial v(\xi)}{\partial t}\right)^2 + \left(\frac{\partial w(\xi)}{\partial t}\right)^2\right]R\left(1 + \frac{\xi}{R}\right)\mathrm{d}\beta\,\mathrm{d}\xi, \tag{19}$$

where ρ is the material density, and $v(\xi)$ and $w(\xi)$ are the tangential and normal displacements of a point on the parallel surface separated from the middle surface by a distance ξ [14], given by

$$v(\xi) = v + \xi\varphi, \qquad w(\xi) = w, \tag{20, 21}$$

where

$$\varphi = -\frac{1}{R}\frac{\partial w}{\partial\beta} + \frac{v}{R}. \tag{22}$$

Substituting equations (20)–(22) into equation (19) and neglecting 4th and higher powers of h_ξ^+ and h_ξ^-, the kinetic energy can be expressed as follows:

$$T = \frac{r_a^4 \rho L}{2}\int_{\beta_1}^{\beta_2}\left\{\left[\left(\frac{\partial v}{\partial t}\right)^2 + \left(\frac{\partial w}{\partial t}\right)^2\right]RH + \left[3\left(\frac{\partial v}{\partial t}\right)^2 - 4\frac{\partial v}{\partial t}\frac{\partial^2 w}{\partial t\,\partial\beta} + \left(\frac{\partial^2 w}{\partial t\,\partial\beta}\right)^2\right]\frac{1}{3R}H^3\right\}\mathrm{d}\beta, \tag{23}$$

in which the terms of the form: $\int_{\beta_1}^{\beta_2} F(\beta)[h_\xi^{+2} - h_\xi^{-2}]\,\mathrm{d}\beta$ have been set to zero in equation (23). The first term on the right-hand side of equation (23) represents

kinetic energy due to the linear velocities of point P on the middle surface and the second term is related to the effect of rotational inertia about the point P.

Having established the appropriate energy expressions it is now necessary to define the generalized co-ordinates which are to be used to define the ring displacements, as outlined in the following section.

4. DISPLACEMENT FUNCTIONS AND CO-ORDINATE TRANSFORMATION

For free vibration at frequency ω the tangential and normal displacements, v and w, of the middle surface are assumed to have the following forms

$$v = \sum_{n=0}^{N} (v_n^s \sin n\beta' - v_n^c \cos n\beta') \, e^{i\omega t}, \tag{24}$$

$$w = \sum_{n=0}^{N} (w_n^c \cos n\beta' + w_n^s \sin n\beta') \, e^{i\omega t}, \tag{25}$$

where v_n^c, v_n^s, w_n^c and w_n^s are the generalized co-ordinates (undetermined amplitude coefficients). The superscripts s and c in equations (24) and (25) denote the coefficients of sine and cosine terms, respectively. It is obvious from equations (24) and (25) that the terms involving v_n^s and w_n^s equal zero when $n = 0$. Thus, one displacement pattern at $n = 0$ is the so-called breathing mode (i.e., radial displacement w is equal at all circumferential positions and the tangential displacement v is zero everywhere), and the other is a rigid body rotation about the ring axis (i.e., the radial displacement w is zero everywhere).

The number of terms to be used in the displacement function series will depend on the degree of accuracy required in the solution. This matter is discussed in further detail in reference [18] when specific examples are investigated.

Note that the strain energy, equation (18), and the kinetic energy, equation (23), are both expressed in terms of the local co-ordinates β, ξ and and tangential and normal displacement components, v and w, integrated over the local tangential co-ordinate β. In order to calculate the natural frequencies (eigenvalues) and the mode shapes (eigenvectors), the displacement functions, v and w, in equation (24) are expressed in terms of global circumferential co-ordinate β'. Hence, it is necessary to make a co-ordinate transformation in equations (18) and (23) to express the local tangential co-ordinate β in terms of the global co-ordinate β'. The integrals can then be evaluated numerically over the global circumferential co-ordinate β' from 0 to 2π.

The required relationship between the global and local co-ordinates can be deduced from Figure 4. This shows the inner and outer profiles and the mid-surface which are defined relative to C'. R is the radius of curvature of the mid-surface at point P. The length ds from P to P' can be expressed as:

$$ds = L_p \, d\beta' = R \, d\beta, \tag{26}$$

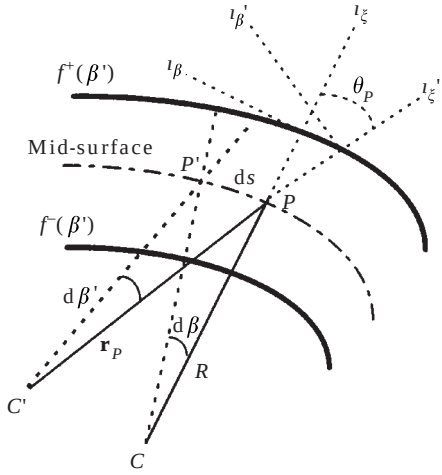

Figure 4. Transformation between global and local co-ordinates.

where L_p is the Lamé's parameter [14], defined as:

$$L_p^2 = \left(\frac{\partial x}{\partial \beta'}\right)^2 + \left(\frac{\partial y}{\partial \beta'}\right)^2. \tag{27}$$

x and y in equation (27) denote generalized representations in the perspective of a curved surface in plane Cartesian co-ordinates.

It follows that

$$d\beta = \frac{L_P}{R}\, d\beta'. \tag{28}$$

Hence

$$\frac{\partial v}{\partial \beta} = \frac{R}{L_p}\frac{\partial v}{\partial \beta'}, \qquad \frac{\partial w}{\partial \beta} = \frac{R}{L_p}\frac{\partial w}{\partial \beta'} \tag{29, 30}$$

and

$$\frac{\partial^2 v}{\partial \beta^2} = \frac{R^2}{L_p^2}\frac{\partial^2 v}{\partial \beta'^2} + \frac{R}{L_p}\frac{\partial v}{\partial \beta'}\left\{R\frac{\partial}{\partial \beta'}\left(\frac{1}{L_P}\right) - \frac{R^2}{L_P}\frac{\partial}{\partial \beta'}\left(\frac{1}{R}\right)\right\}, \tag{31}$$

$$\frac{\partial^2 w}{\partial \beta^2} = \frac{R^2}{L_p^2}\frac{\partial^2 w}{\partial \beta'^2} + \frac{R}{L_p}\frac{\partial w}{\partial \beta'}\left\{R\frac{\partial}{\partial \beta'}\left(\frac{1}{L_p}\right) - \frac{R^2}{L_p}\frac{\partial}{\partial \beta'}\left(\frac{1}{R}\right)\right\}. \tag{32}$$

Substituting equations (28)–(32) into equations (18) and (23), the strain and kinetic energies can be rewritten in terms of the global co-ordinate β', integrated from 0 to 2π as follows:

$$S = \frac{r_a^2 EL}{2}\int_0^{2\pi}\left\{\frac{L_p}{R^2}\left[\frac{R^2}{L_p^2}\left(\frac{\partial v}{\partial \beta'}\right) + 2\,\frac{R}{L_p}\,w\,\frac{\partial v}{\partial \beta'} + w^2\right]H\right.$$

$$+\frac{L_p}{3R^4}\left[w^2 + 2\,\frac{R^2}{L_p^2}\,w\,\frac{\partial^2 w}{\partial \beta'^2} + \frac{R^4}{L_p^4}\left(\frac{\partial^2 w}{\partial \beta'^2}\right)^2\right]H^3$$

$$+\frac{2}{3R^2}\left[w\,\frac{\partial w}{\partial \beta'} + \frac{R^2}{L_p^2}\,\frac{\partial w}{\partial \beta'}\,\frac{\partial^2 w}{\partial \beta'^2}\right]\frac{\partial}{\partial \beta'}\left(\frac{1}{L_p}\right)H^3$$

$$-\frac{2}{3R^2}\left[vw + \frac{R^2}{L_p^2}\,v\,\frac{\partial^2 w}{\partial \beta'^2}\right]\frac{\partial}{\partial \beta'}\left(\frac{1}{R}\right)H^3$$

$$+\frac{1}{3L_p}\left(\frac{\partial w}{\partial \beta'}\right)^2\left[\frac{\partial}{\partial \beta'}\left(\frac{1}{L_p}\right)\right]^2 H^3$$

$$+\frac{1}{3L_p}\,v^2\left[\frac{\partial}{\partial \beta'}\left(\frac{1}{R}\right)\right]^2 H^3$$

$$\left.-\frac{2}{3L_p}\,v\,\frac{\partial w}{\partial \beta'}\left[\frac{\partial}{\partial \beta'}\left(\frac{1}{R}\right)\frac{\partial}{\partial \beta'}\left(\frac{1}{L_p}\right)\right]H^3\right\}\mathrm{d}\beta', \tag{33}$$

$$T = \frac{r_a^4 \rho L}{2}\int_0^{2\pi}\left\{L_p\left[\left(\frac{\partial v}{\partial t}\right)^2 + \left(\frac{\partial w}{\partial t}\right)^2\right]H\right.$$

$$\left.+\frac{L_p}{3R^2}\left[3\left(\frac{\partial v}{\partial t}\right)^2 - \frac{4R}{L_p}\,\frac{\partial v}{\partial t}\,\frac{\partial^2 w}{\partial t\,\partial \beta'} + \frac{R^2}{L_p^2}\left(\frac{\partial^2 w}{\partial t\,\partial \beta'}\right)^2\right]H^3\right\}\mathrm{d}\beta'. \tag{34}$$

5. EIGENVALUE PROBLEM

Making use of the results derived in the previous sections of the paper, the Rayleigh–Ritz procedure can now be applied to obtain the eigenvalue problem which can be expressed in the following general matrix form

$$\left[\begin{bmatrix}\mathbf{K}^{ss} & \mathbf{K}^{sc}\\ \mathbf{K}^{cs} & \mathbf{K}^{cc}\end{bmatrix} - \lambda^2\begin{bmatrix}\mathbf{M}^{ss} & \mathbf{M}^{sc}\\ \mathbf{M}^{cs} & \mathbf{M}^{cc}\end{bmatrix}\right]\begin{bmatrix}\mathbf{q}_s\\ \mathbf{q}_c\end{bmatrix} = \begin{bmatrix}\mathbf{0}\\ \mathbf{0}\end{bmatrix}, \tag{35}$$

where

$$\mathbf{q}_s = \begin{bmatrix} v_0^s \\ w_0^s \\ v_1^s \\ w_1^s \\ \vdots \\ \vdots \\ v_N^s \\ w_N^s \end{bmatrix}, \qquad \mathbf{q}_c = \begin{bmatrix} v_0^c \\ w_0^c \\ v_1^c \\ w_1^c \\ \vdots \\ \vdots \\ v_N^c \\ w_N^c \end{bmatrix} \tag{36}$$

and $[\mathbf{K}^{ss}]$ etc. and $[\mathbf{M}^{ss}]$ etc. represent stiffness and mass matrices of size $2(N+1)$, where N is the number of terms in the displacement function series (equations (24) and (25)). The matrix elements are given in the Appendix. The superscripts s and c indicate that the coefficients are related to sine and cosine terms, respectively, in the displacement function series and $\mathbf{q}_s, \mathbf{q}_c$ are vectors of generalised co-ordinates v_n, w_n. The frequency factors of the ring, λ, are the eigenvalues of equation (35) (calculated using standard NAG routines) and are defined by

$$\lambda_n = \sqrt{\frac{\rho}{E}}\,\omega_n r_a, \tag{37}$$

where ω_n is the natural frequency of the nth radial mode.

For a given value of n, equation (37) will yield a pair of values of λ_n. These will be equal in the case of a perfect ring but will be different in the case of an imperfect ring, giving rise to a higher frequency mode and a lower frequency mode for each value of n. The magnitude of the frequency splitting between a given pair of modes will often be small, of the order of a fraction of 1% of the nominal value. Sometimes, however, for particular combinations of profile variation and mode number, the frequency splitting can be much larger, of the order of 20% or 30% [7, 18].

In the general case where the profile of the ring is not symmetric with respect to $\beta' = 0$, the frequently used classification of the modes as being "symmetric" and "anti-symmetric" would be inappropriate. In the special cases where the ring is either perfectly circular or is symmetric about the line defined by $\beta' = 0$, the off-diagonal sub-matrices $[\mathbf{K}^{sc}]$, $[\mathbf{K}^{cs}]$, $[\mathbf{M}^{sc}]$ and $[\mathbf{M}^{cs}]$ appearing in equation (35) will be null matrices. In this case equation (35) decomposes into two uncoupled sets of equations: one set would give modes which are symmetric with respect to $\beta' = 0$ and the other would give modes which are anti-symmetric.

It should be noted that in solving equation (35) the generalised co-ordinates v_0^s and w_0^s are set to zero to eliminate rigid body motions. In order to get non-trivial results, all the corresponding columns and rows of the mass and stiffness matrices which correspond to v and $\partial/\partial v$ at $n = 0$, and w and $\partial/\partial w$ at $n = 0$, which are zero, must be removed.

6. CONCLUSIONS

This paper presents a methodology and formulation of the eigenvalue problem for the free, in-plane, vibration of thin rings of rectangular cross-section and circumferential profile variation. The profiles of the outer and inner surfaces of the ring are expressed, in a general way, by Fourier series. An iterative numerical procedure is presented for the proper determination of the true middle surface from the specified outer and inner surfaces of the ring. This procedure allows rings of arbitrary shape to be dealt with. General expressions are presented for the corresponding mass and stiffness matrices. The resulting eigenvalue problem can be solved using standard procedures. A companion paper [18] presents a comprehensive set of results relating to applications of the theory to rings of nominally circular shape and a further paper [19] presents results for rings of nominally elliptical shape.

REFERENCES

1. A. E. H. Love 1944 *A Treatise on the Mathematical Theory of Elasticity*. New York: Dover; 4th edition.
2. A. W. Leissa 1973 *Vibration of Shells*. NASA, SP-288. U.S. Government Printing Office. Reprinted by *The Acoustical Society of America* in 1993.
3. S. A. Tobias 1957 *Engineering*, 409–410. A theory of imperfection for elastic bodies of revolution.
4. C. H. J. Fox 1988 *Proceeding of DGON Symposium on Gyro Technology Stuttgart, Germany*. Vibrating cylinder rate gyro: theory of operation and error analysis.
5. C. H. J. Fox 1990 *Journal of Sound and Vibration* **142**, 227–243. A simple theory for the analysis and correction of frequency splitting in slightly imperfect rings.
6. R. Hoppe 1871 *Crelle Journal of Mathematics* **73**, 158–170. The bending vibration of a circular ring.
7. R. S. Hwang 1997 *Ph.D. Thesis, University of Nottingham, U.K.* Free vibrations of a thin ring having circumferential profile variations.
8. P. Chidamparam and A. W. Leissa 1993 *Applied Mechanics Review* **46**, 467–483. Vibrations of planar curved beams, rings and arches.
9. K. Suzuki and A. W. Leissa 1985 *ASME Journal of Applied Mechanics* **52**, 149–154. Free vibration on non-circular cylindrical shells having circumferentially varying thickness.
10. K. Suzuki and A. W. Leissa 1986 *Journal of Sound and Vibration* **107**, 1–15. Exact solutions for the free vibrations of open cylindrical shells with circumferentially varying curvature and thickness.
11. C. P. Filipich, P. A. A. Laura, M. Rosales and B. H. Valerga de Greco 1987 *Journal of Sound and Vibration* **118**, 166–169. Numerical experiments on in-plane vibrations of rings of non-uniform cross section.
12. P. A. A. Laura, C. P. Filipich, R. E. Rossi and J. A. Reyes 1988 *Applied Acoustics* **25**, 225–234. Vibrations of rings of variable cross-section.
13. T. P. Valkering and T. Charnley 1983 *Journal of Sound and Vibration* **86**, 369–393. Radial vibrations of eccentric rings.
14. R. F. Tonin and D. A. Bies 1979 *Journal of Sound and Vibration* **62**, 165–180. Free vibration of circular cylinders of variable thickness.
15. V. V. Novozhilov 1959 *The Theory of Thin Shells*. Grönigen: Noordhoff; 1st edition.
16. G. B. Warburton 1969 *Proceedings of the Symposium on Structural Dynamics*. University of Loughbourough, U.K. Vol 1, a1.1–a1.34. Dynamics of shells.

17. W. T. KOITER 1967 *IUTAM Symposium on Dynamics of Shells*, 93–105. Foundations and basic equations of shell theory: a survey of recent progress.
18. C. H. J. FOX, R. S. HWANG and S. MCWILLIAM 1999 *Journal of Sound and Vibration* **220,** 517–539. The in-plane vibration of thin rings with in-plane profile variations Part II: application to nominally circular rings.
19. S. MCWILLIAM, R. S. HWANG and C. H. J. FOX 1998 *Journal of Sound and Vibration* (submitted). Free vibration of elliptical rings with circumferentially variable thickness.
20. E. KREYSZIG 1983 *Advanced Engineering Mathematics*. Singapore: Wiley; 6th edition. See p. 476.

APPENDIX: MATRIX ELEMENTS IN THE FREQUENCY EQUATION

The elements of the stiffness and mass matrices in equation (35) can be expressed as follows where m and n are integers which take on the range of values from 0 to N, where N is the number of terms of the displacement function series. Note that the variables m, n used in this Appendix have different meanings from those in the main body of the paper.

(i) The elements of the stiffness matrix

$$\mathbf{K}[m+1, n+1] = mnB_4 + \tfrac{1}{3}A_{11},$$

$$\mathbf{K}[m+1, n+N+2] = mB_3 + \tfrac{1}{3}[n^2D_{17} - D_{14} + nA_{13}],$$

$$\mathbf{K}[m+1, n+2N+3] = mnC_4 - \tfrac{1}{3}D_{11},$$

$$\mathbf{K}[m+1, n+3N+4] = mC_3 + \tfrac{1}{3}[n^2A_{17} - A_{14} - nD_{13}],$$

$$\mathbf{K}[m+N+2, n+1] = nB_3 + \tfrac{1}{3}[m^2C_{17} - C_{14} + mA_{13}],$$

$$\mathbf{K}[m+N+2, n+N+2] = B_2 + \tfrac{1}{3}[B_6 - (m^2+n^2)B_9 + m^2n^2B_{10} - nC_{15} + nm^2C_{16} - mD_{15} + mn^2D_{16} + mnA_{12}],$$

$$\mathbf{K}[m+N+2, n+2N+3] = nC_3 + \tfrac{1}{3}[B_{14} - m^2B_{17} - mD_{13}],$$

$$\mathbf{K}[m+N+2, n+3N+4] = C_2 + \tfrac{1}{3}[C_6 - (m^2+n^2)C_9 + m^2n^2C_{10} + nB_{15} - nm^2B_{16} - mA_{15} + mn^2A_{16} - mnD_{12}],$$

$$\mathbf{K}[m+2N+3, n+1] = nmD_4 - \tfrac{1}{3}C_{11},$$

$$\mathbf{K}[m+2N+3, n+N+2] = mD_3 + \tfrac{1}{3}[B_{14} - n^2B_{17} - nC_{13}],$$

$$\mathbf{K}[m+2N+3, n+2N+3] = mnA_{14} + \tfrac{1}{3}B_{11},$$

$$\mathbf{K}[m+2N+3, n+3N+4] = mA_3 + \tfrac{1}{3}[C_{14} - n^2C_{17} + nB_{13}],$$

$$\mathbf{K}[m+3N+4, n+1] = nD_3 + \tfrac{1}{3}[m^2A_{17} - A_{14} - mC_{13}],$$

$$\mathbf{K}[m+3N+4, n+N+2] = D_2 + \tfrac{1}{3}[D_6 - (m^2+n^2)D_9 + m^2n^2D_{10} + mB_{15} - mn^2B_{16} - nA_{15} + nm^2A_{16} - mnC_{12}],$$

$$\mathbf{K}[m+3N+4, n+2N+3] = nA_3 + \tfrac{1}{3}[D_{14} - m^2D_{17} + mB_{13}],$$

$$\mathbf{K}[m+3N+4, n+3N+4] = A_2 + \tfrac{1}{3}[A_6 - (m^2+n^2)A_9 + m^2n^2A_{10} + nD_{15} - nm^2D_{16} + mC_{15} - mn^2C_{16} + mnB_{12}].$$

(ii) The elements of the mass matrix

$$\mathbf{M}[m+1, n+1] = A_1 + A_5, \qquad \mathbf{M}[m+1, n+N+2] = \tfrac{2}{3}nA_7,$$

$$\mathbf{M}[m+1, n+2N+3] = -D_1 - D_5, \qquad \mathbf{M}[m+1, n+3N+4] = -\tfrac{2}{3}nD_7,$$

$$\mathbf{M}[m+N+2, n+1] = \tfrac{2}{3}mA_7, \qquad \mathbf{M}[m+N+2, n+N+2] = B_1 + \tfrac{1}{3}mnA_8,$$

$$\mathbf{M}[m+N+2, n+2N+3] = -\tfrac{2}{3}mD_7,$$

$$\mathbf{M}[m+N+2, n+3N+4] = C_1 - \tfrac{1}{3}mnD_8,$$

$$\mathbf{M}[m+2N+3, n+1] = -C_1 - C_5, \qquad \mathbf{M}[m+2N+3, n+N+2] = -\tfrac{2}{3}nC_7,$$

$$\mathbf{M}[m+2N+3, n+2N+3] = B_1 + B_5, \qquad \mathbf{M}[m+2N+3, n+3N+4] = \tfrac{2}{3}nB_7,$$

$$\mathbf{M}[m+3N+4, n+1] = -\tfrac{2}{3}mC_7, \qquad \mathbf{M}[m+3N+4, n+N+2] = D_1 - \tfrac{1}{3}mnC_8,$$

$$\mathbf{M}[m+3N+4, n+2N+3] = \tfrac{2}{3}mB_7,$$

$$\mathbf{M}[m+3N+4, n+3N+4] = A_1 + \tfrac{1}{3}mnB_8.$$

In the following expressions, L_p denotes Lamé's parameter, R denotes the radius of curvatures, $\Gamma^{ij}_{kl} = \cos(i\beta')\cos(j\beta')\sin(k\beta')\sin(l\beta')$, and H and H^3 denote $(h^+ - h^-)$ and $(h^{+3} - h^{-3})$, respectively, where h^+ and h^- are the outer and inner thicknesses, respectively. These variables can be calculated by an iterative numerical procedure shown in the main text.

$$A_1 = \int_0^{2\pi} L_p \Gamma_{mn} H \, \mathrm{d}\beta', \qquad B_1 = \int_0^{2\pi} L_p \Gamma^{mn} H \, \mathrm{d}\beta',$$

$$A_2 = \int_0^{2\pi} \frac{L_p}{R^2} \Gamma_{mn} H \, \mathrm{d}\beta', \qquad B_2 = \int_0^{2\pi} \frac{L_p}{R^2} \Gamma^{mn} H \, \mathrm{d}\beta',$$

$$A_3 = \int_0^{2\pi} \frac{1}{R} \Gamma_{mn} H \, \mathrm{d}\beta', \qquad B_3 = \int_0^{2\pi} \frac{1}{R} \Gamma^{mn} H \, \mathrm{d}\beta',$$

$$A_4 = \int_0^{2\pi} \frac{1}{L_p} \Gamma_{mn} H \, \mathrm{d}\beta', \qquad B_4 = \int_0^{2\pi} \frac{1}{L_p} \Gamma^{mn} H \, \mathrm{d}\beta',$$

$$A_5 = \int_0^{2\pi} \frac{L_p}{R^2} \Gamma_{mn} H^3 \, \mathrm{d}\beta', \qquad B_5 = \int_0^{2\pi} \frac{L_p}{R^2} \Gamma^{mn} H^3 \, \mathrm{d}\beta',$$

$$A_6 = \int_0^{2\pi} \frac{L_p}{R^4} \Gamma_{mn} H^3 \, \mathrm{d}\beta', \qquad B_6 = \int_0^{2\pi} \frac{L_p}{R^4} \Gamma^{mn} H^3 \, \mathrm{d}\beta',$$

$$A_7 = \int_0^{2\pi} \frac{1}{R} \Gamma_{mn} H^3 \, \mathrm{d}\beta', \qquad B_7 = \int_0^{2\pi} \frac{1}{R} \Gamma^{mn} H^3 \, \mathrm{d}\beta',$$

$$A_8 = \int_0^{2\pi} \frac{1}{L_p} \Gamma_{mn} H^3 \, \mathrm{d}\beta', \qquad B_8 = \int_0^{2\pi} \frac{1}{L_p} \Gamma^{mn} H^3 \, \mathrm{d}\beta',$$

$$A_9 = \int_0^{2\pi} \frac{1}{L_p R^2} \Gamma_{mn} H^3 \, \mathrm{d}\beta', \qquad B_9 = \int_0^{2\pi} \frac{1}{L_p R^2} \Gamma^{mn} H^3 \, \mathrm{d}\beta',$$

$$A_{10} = \int_0^{2\pi} \frac{L_p^3}{\Gamma_{mn} H^3 \, \mathrm{d}\beta'}, \qquad B_{10} = \int_0^{2\pi} \frac{1}{L_p^3} \Gamma^{mn} H^3 \, \mathrm{d}\beta',$$

$$A_{11} = \int_0^{2\pi} \frac{1}{L_p} \left(\frac{\partial}{\partial \beta'} \left(\frac{1}{R} \right) \right)^2 \Gamma_{mn} H^3 \, \mathrm{d}\beta', \qquad \beta_{11} = \int_0^{2\pi} \frac{1}{L_p} \left(\frac{\partial}{\partial \beta'} \left(\frac{1}{R} \right) \right)^2 \Gamma^{mn} H^3 \, \mathrm{d}\beta',$$

$$A_{12} = \int_0^{2\pi} \frac{1}{L_p} \left(\frac{\partial}{\partial \beta'} \left(\frac{1}{L_p} \right) \right)^2 \Gamma_{mn} H^3 \, \mathrm{d}\beta', \qquad B_{12} = \int_0^{2\pi} \frac{1}{L_p} \left(\frac{\partial}{\partial \beta'} \left(\frac{1}{L_p} \right) \right)^2 \Gamma^{mn} H^3 \, \mathrm{d}\beta',$$

$$A_{13} = \int_0^{2\pi} \frac{1}{L_p} \frac{\partial}{\partial \beta'} \left(\frac{1}{R} \right) \frac{\partial}{\partial \beta'} \left(\frac{1}{L_p} \right) \Gamma_{mn} H^3 \, \mathrm{d}\beta',$$

$$B_{13} = \int_0^{2\pi} \frac{1}{L_p} \frac{\partial}{\partial \beta'} \left(\frac{1}{R} \right) \frac{\partial}{\partial \beta'} \left(\frac{1}{L_p} \right) \Gamma^{mn} H^3 \, \mathrm{d}\beta',$$

$$A_{14} = \int_0^{2\pi} \frac{1}{R^2} \frac{\partial}{\partial \beta'} \left(\frac{1}{R} \right) \Gamma_{mn} H^3 \, \mathrm{d}\beta', \qquad B_{14} = \int_0^{2\pi} \frac{1}{R^2} \frac{\partial}{\partial \beta'} \left(\frac{1}{R} \right) \Gamma^{mn} H^3 \, \mathrm{d}\beta',$$

$$A_{15} = \int_0^{2\pi} \frac{1}{R^2} \frac{\partial}{\partial \beta'} \left(\frac{1}{L_p} \right) \Gamma_{mn} H^3 \, \mathrm{d}\beta', \qquad B_{15} = \int_0^{2\pi} \frac{1}{R^2} \frac{\partial}{\partial \beta'} \left(\frac{1}{L_p} \right) \Gamma^{mn} H^3 \, \mathrm{d}\beta',$$

$$A_{16} = \int_0^{2\pi} \frac{1}{L_p^2} \frac{\partial}{\partial \beta'} \left(\frac{1}{L_p} \right) \Gamma_{mn} H^3 \, \mathrm{d}\beta', \qquad B_{16} = \int_0^{2\pi} \frac{1}{L_p^2} \frac{\partial}{\partial \beta'} \left(\frac{1}{L_p} \right) \Gamma^{mn} H^3 \, \mathrm{d}\beta',$$

$$A_{17} = \int_0^{2\pi} \frac{1}{L_p^2} \frac{\partial}{\partial \beta'} \left(\frac{1}{R} \right) \Gamma_{mn} H^3 \, \mathrm{d}\beta', \qquad B_{17} = \int_0^{2\pi} \frac{1}{L_p^2} \frac{\partial}{\partial \beta'} \left(\frac{1}{R} \right) \Gamma^{mn} H^3 \, \mathrm{d}\beta',$$

$$C_1 = \int_0^{2\pi} L_p \Gamma_n^m H \, \mathrm{d}\beta', \qquad D_1 = \int_0^{2\pi} L_p \Gamma_m^n H \, \mathrm{d}\beta',$$

$$C_2 = \int_0^{2\pi} \frac{L_p}{R^2} \Gamma_n^m H \, \mathrm{d}\beta', \qquad D_2 = \int_0^{2\pi} \frac{L_p}{R^2} \Gamma_m^n H \, \mathrm{d}\beta',$$

$$C_3 = \int_0^{2\pi} \frac{1}{R}\,\Gamma_n^m H\,\mathrm{d}\beta', \qquad D_3 = \int_0^{2\pi} \frac{1}{R}\,\Gamma_m^n H\,\mathrm{d}\beta',$$

$$C_4 = \int_0^{2\pi} \frac{1}{L_p}\,\Gamma_n^m H\,\mathrm{d}\beta', \qquad D_4 = \int_0^{2\pi} \frac{1}{L_p}\,\Gamma_m^n H\,\mathrm{d}\beta',$$

$$C_5 = \int_0^{2\pi} \frac{L_p}{R^2}\,\Gamma_n^m H^3\,\mathrm{d}\beta', \qquad D_5 = \int_0^{2\pi} \frac{L_p}{R^2}\,\Gamma_m^n H^3\,\mathrm{d}\beta',$$

$$C_6 = \int_0^{2\pi} \frac{L_p}{R^4}\,\Gamma_n^m H^3\,\mathrm{d}\beta', \qquad D_6 = \int_0^{2\pi} \frac{L_p}{R^4}\,\Gamma_m^n H^3\,\mathrm{d}\beta',$$

$$C_7 = \int_0^{2\pi} \frac{1}{R^2}\,\Gamma_n^m H^3\,\mathrm{d}\beta', \qquad D_7 = \int_0^{2\pi} \frac{1}{R^2}\,\Gamma_m^n H^3\,\mathrm{d}\beta',$$

$$C_8 = \int_0^{2\pi} \frac{1}{L_p}\,\Gamma_n^m H^3\,\mathrm{d}\beta', \qquad D_8 = \int_0^{2\pi} \frac{1}{L_p}\,\Gamma_m^n H^3\,\mathrm{d}\beta',$$

$$C_9 = \int_0^{2\pi} \frac{1}{L_p R^2}\,\Gamma_n^m H^3\,\mathrm{d}\beta', \qquad D_9 = \int_0^{2\pi} \frac{1}{L_p R^2}\,\Gamma_m^n H^3\,\mathrm{d}\beta',$$

$$C_{10} = \int_0^{2\pi} \frac{1}{L_p^3}\,\Gamma_n^m H^3\,\mathrm{d}\beta', \qquad D_{10} = \int_0^{2\pi} \frac{1}{L_p^3}\,\Gamma_m^n H^3\,\mathrm{d}\beta',$$

$$C_{11} = \int_0^{2\pi} \frac{1}{L_p}\left(\frac{\partial}{\partial\beta'}\left(\frac{1}{R}\right)\right)^2 \Gamma_n^m H^3\,\mathrm{d}\beta', \qquad D_{11} = \int_0^{2\pi} \frac{1}{L_p}\left(\frac{\partial}{\partial\beta'}\left(\frac{1}{R}\right)\right)^2 \Gamma_m^n H^3\,\mathrm{d}\beta',$$

$$C_{12} = \int_0^{2\pi} \frac{1}{L_p}\left(\frac{\partial}{\partial\beta'}\left(\frac{1}{L_p}\right)\right)^2 \Gamma_n^m H^3\,\mathrm{d}\beta', \qquad D_{12} = \int_0^{2\pi} \frac{1}{L_p}\left(\frac{\partial}{\partial\beta'}\left(\frac{1}{L_p}\right)\right)^2 \Gamma_m^n H^3\,\mathrm{d}\beta',$$

$$C_{13} = \int_0^{2\pi} \frac{1}{L_p}\frac{\partial}{\partial\beta'}\left(\frac{1}{R}\right)\frac{\partial}{\partial\beta'}\left(\frac{1}{L_p}\right)\Gamma_n^m H^3\,\mathrm{d}\beta',$$

$$D_{13} = \int_0^{2\pi} \frac{1}{L_p}\frac{\partial}{\partial\beta'}\left(\frac{1}{R}\right)\frac{\partial}{\partial\beta'}\left(\frac{1}{L_p}\right)\Gamma_m^n H^3\,\mathrm{d}\beta',$$

$$C_{14} = \int_0^{2\pi} \frac{1}{R^2}\frac{\partial}{\partial\beta'}\left(\frac{1}{R}\right)\Gamma_n^m H^3\,\mathrm{d}\beta', \qquad D_{14} = \int_0^{2\pi} \frac{1}{R^2}\frac{\partial}{\partial\beta'}\left(\frac{1}{R}\right)\Gamma_m^n H^3\,\mathrm{d}\beta',$$

$$C_{15} = \int_0^{2\pi} \frac{1}{R^2} \frac{\partial}{\partial \beta'} \left(\frac{1}{L_p} \right) \Gamma_n^m H^3 \, \mathrm{d}\beta', \qquad D_{15} = \int_0^{2\pi} \frac{1}{R^2} \frac{\partial}{\partial \beta'} \left(\frac{1}{L_p} \right) \Gamma_m^n H^3 \, \mathrm{d}\beta',$$

$$C_{16} = \int_0^{2\pi} \frac{1}{L_p^2} \frac{\partial}{\partial \beta'} \left(\frac{1}{L_p} \right) \Gamma_n^m H^3 \, \mathrm{d}\beta', \qquad D_{16} = \int_0^{2\pi} \frac{1}{L_p^2} \frac{\partial}{\partial \beta'} \left(\frac{1}{L_p} \right) \Gamma_m^n H^3 \, \mathrm{d}\beta',$$

$$C_{17} = \int_0^{2\pi} \frac{1}{L_p^2} \frac{\partial}{\partial \beta'} \left(\frac{1}{R} \right) \Gamma_n^m H^3 \, \mathrm{d}\beta', \qquad D_{17} = \int_0^{2\pi} \frac{1}{L_p^2} \frac{\partial}{\partial \beta'} \left(\frac{1}{R} \right) \Gamma_m^n H^3 \, \mathrm{d}\beta'.$$